ISBN: 978-3-95450-261-5 ISSN: 2673-7000 doi: 10.18429/JACoW-NAPAC2025-WEP049

PROGRESS REPORT ON TWO-BUNCH EXCITATION OF WAKEFIELD IN DIELECTRIC STRUCTURES*

C. Phillips†[1], B. Leung[1], X. Lu[1,2], P. Piot[2], E. Wisniewski[2],
J. Power[2], S. Doran[2], E. Gomez[3], L. Stan[2]
[1] Northern Illinois University, DeKalb, IL, USA
[2] Argonne National Laboratory, Lemont, IL, USA
[3] Euclid Techlabs, Bolingbrook, IL, USA

Abstract

Wakefield accelerators have the potential to achieve accelerating fields in the GV/m range, offering a promising path to more compact and cost-effective acceleration compared to conventional methods. Structure-based wakefield accelerator (SWFA) technology provides a viable approach to implementing beam-driven wakefield acceleration. An experiment at the Argonne Wakefield Accelerator (AWA) will utilize dielectric-lined structures to explore multi-beam excitation of wakefields for wakefield-pulse shortening and mapping of the transverse wakefield topology. These structures were commercially sourced and require a thin metallic film deposited on their outer surface. The first part of this paper summarizes the preparation of these structures. In parallel, a two-bunch beam configuration is required to support the experimental investigation, where one bunch excites the wakefield and the second serves as a loading or probe bunch. The experimental generation and testing of this two-bunch scheme at AWA are presented in this work.

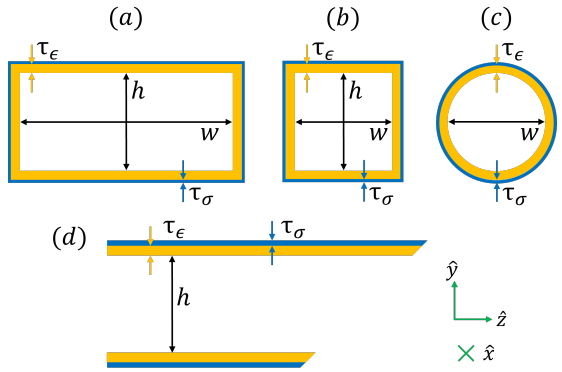

Figure 1: Cross-sectional views [in (x, y) plane] of the rectangular (a), square (b), and circular (c) structures along with longitudinal (y, z) slice of the angled cut circular structure for 35°. The structures have an inner height h, width w, dielectric thickness τ_ϵ, and conductor coating thickness of τ_σ, and all have the same length along the z direction. The shaded areas and dark lines represent the dielectric material and the metallic layer on its outer surface, respectively.

INTRODUCTION

Wakefields are produced by charged particles traveling between two or more dielectric surfaces. By carefully tailoring how they are produced, we are able to create localized regions of high energy gradients that can be used to accelerate a following bunch. This process, referred to as dielectric wakefield acceleration (DWFAs), has significantly higher gradients than standard RF cavities and has been studied using circular [1, 2] and slab structures [3, 4]. DWFA is a sub class for structure wakefield acceleration (SWFA) being explored for next-generation energy-frontier collider [5] or compact future light source [6, 7]. This process employs a high-charge "drive" bunch that creates the wake and a lower-charged "witness" bunch that experiences acceleration. An appealing development is to recycle the wake from a drive bunch.

The planned experiment will especially test whether a properly delayed "loading" bunch can suppress the wake generated by the drive bunch, enabling accurate characterization of the field for potential energy recovery. At the Argonne Wakefield Accelerator (AWA) facility, this will be implemented using same-charge dual-bunch excitation of dielectric-wakefield accelerators (DWFAs). The approach has two main components: (1) a properly delayed loading bunch, and (2) a dielectric structure with a non-90° cut at the exit (Fig. 1(d)), allowing the particles to continue straight while the radiation travels at an angle to be studied.

To investigate the influence of geometry and ,e.g., possibly control of transverse wakefield [8], three dielectric structures with different cross-sectional geometries - circle, square, and rectangle - have been prepared (Fig. 1(a-c)). These geometries are expected to affect the wakefield behavior, especially to suppress unwanted fields and identify loci of zero transverse force [9]. This paper describes the experimental setup, configuration, and preliminary results from the two-bunch tests.

Additionally, this paper describes the metallic coating applied to the outer surfaces of the dielectric structures. To prevent electromagnetic fields from propagating through the structures' side walls, the metallic layer must be 2–3 times the skin depth δ_s. For frequencies within [70, 140] GHz,

* The work performed at the Center for Nanoscale Materials was supported by the U.S. Department of Energy (DOE), Office of Basic Energy Sciences, under Contract No. DE-AC02-06CH11357. The Argonne Wakefield Accelerator (AWA) is supported by the DOE Office of Science, High Energy Physics, under Contract No. DE-AC02-06CH11357. CP, BL, and in part XL, are supported by DOE Contract No. DE-SC0022010 awarded to Northern Illinois University.
† z1907262@students.niu.edu

ISBN: 978-3-95450-261-5 ISSN: 2673-7000 doi: 10.18429/JACoW-NAPAC2025-WEP049

Table 1: Dimensions associated with the structures shown in Fig. 1. All dimensions, including the fundamental-mode wavelength (λ), are given in millimeters. The skin depth δ_s values are given in nanometers.

structure type	h	w	τ_ϵ	λ	δ_s
rectangle	2	4	0.4	3.68	136
square	2	2	0.4	3.84	139
circle	2	2	0.2	2.09	102

the maximum calculated skin depth is $\delta_s \simeq 140$ nm (see Table 1), resulting in a target coating thickness of 450 nm. The structures, procured from VITROCOM, require thin-film deposition on their outer surfaces. However, due to the small dimensions of the tubes, this process cannot be readily completed externally using standard coating services. Consequently, the deposition was performed in-house using a custom-built deposition chamber at Euclid Techlabs.

THIN-FILM DEPOSITION

While thin-film deposition is widely available commercially for most applications, the dielectric structures for the upcoming wakefield experiment have such small dimensions that a specialized deposition plan had to be enacted. The coatings were applied using Euclid Techlab's custom-built sputtering chamber, which needed to be characterized to determine accurate deposition rates before the coating of the final structures.

In order to quantify the deposition rates of the sputtering chamber we use flatter pieces of glass, ordered from the same manufacturer as the final structures, with a width of 20 mm and cut to lengths of ~150 mm. Three samples were masked lengthwise at the halfway point with aluminum foil and tape, then positioned precisely within the deposition chamber. They were then coated in 10 minute increments, separately, for a total of 10, 20, and 30 minutes. This approach allowed measurement of both the overall deposition rates and its variation with distance from directly under the copper source. Following coating, the samples were measured at the Center for Nanoscale Materials (CNM) at Argonne National Laboratory. A surface profiler was used to measure the step height between the coated and uncoated regions at intervals of 1 ± 0.15 cm along the length of each sample; see Fig. 2.

A notable observation is the pronounced peak in thickness at the center position, which increases significantly with longer deposition times. This confirmed the need to translate the structures during sputtering to achieve a uniform coating. Deposition rate averages for regions farthest from the source (≥12 cm) and for the first 7.05 cm (source center is at 3.525 cm) are summarized in Table 2.

The deposition rate measurements show that, at distances more than 9 cm away from the source center (12+ along the structure lengths), the deposition average thickness is only 33–38% compared to the region under the source. Under

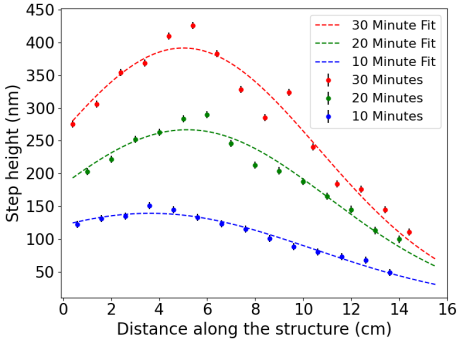

Figure 2: Deposition thickness as a function of length along the structures for three deposition times along with fits to understand the deposition rate fall off farther from the center of the source.

Table 2: Average deposition step from the fits under the center of the source (<7.05 cm in Fig. 2) and far away from the source (>12 cm in Fig. 2). All parameters are in nanometers.

total time	average step <7.05 cm	error ±	average step >12 cm	error ±
10 min	133.8	5.33	46.7	4.9
20 min	246.7	5.34	94.87	5
30 min	361.5	5.28	120.3	4.9

the source, the rate is 12.1 nm/s, compared to 4.19 nm/s in the farthest region. If the structure spends half the time directly under the source and half the time far away from the source, a 55 minute deposition time is required to reach the target thickness of 450 nm. For the final design, a 60-minute deposition was chosen to ensure adequate coverage.

The final procedure incorporated a translation stage and a larger chamber to ensure space for the structure holder. Because of this, additional information had to be considered to determine final deposition time. A large concern was the delamination of the copper from the glass, so a thinner layer of titanium was deposited (10 minute run) before the copper sputtering. This ensures a better adherence of the copper. To further mitigate delamination, the copper source to sample distance was increased from 80 mm (used for the initial tests) to 110 mm for final depositions. The operating pressure was also reduced from 1×10^{-3} to 3×10^{-4} mbar, further minimizing delamination risk. These two changes resulted in slower deposition rates.

These considerations along with the structures positioning led us to opt for an 80-minutes deposition times. During coating, each structure was mounted by its ends to prevent sputtering onto the tube ends or interior. They were also attached to a manual translation stage that was not centered under the source. Because of this, each 10 minute interval consisted of three minutes at one end, three minutes near the structure center, and four minutes at the opposite limit of the stage. This cycle was repeated eight times to achieve the full 80-minute deposition, with three structures processed

ISBN: 978-3-95450-261-5 ISSN: 2673-7000 doi: 10.18429/JACoW-NAPAC2025-WEP049

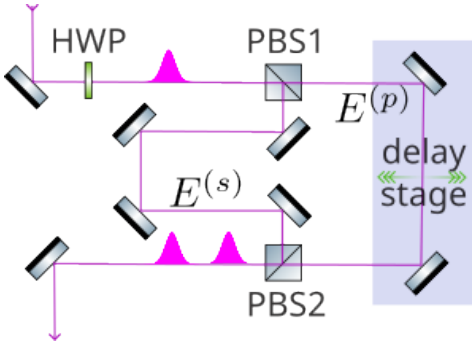

Figure 3: Optical scheme for two-bunch generation using a polarizing splitting/recombining of the UV laser pulse.

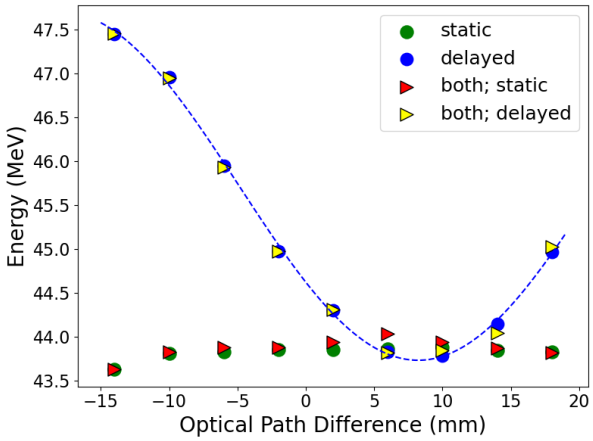

Figure 4: Energy measured using the single bunch configuration ("static", "delayed") and of both bunches simultaneously ("both") as a function of the optical path difference between the *s* and *p*-polarized UV pulses.

simultaneously. After each run, the structures were rotated about 120° to ensure coating uniformity.

After coating, the structures were transferred to a vacuum oven. They were baked at 400°C for two hours. This results in a better adherence of the copper to the titanium and the titanium to the glass, as well as ensuring the baking off of any contaminants before installation into the AWA beamline.

TWO-BUNCH GENERATION

The generation of two electron bunches with a controllable delay was experimentally tested at the AWA using the laser pulse-splitting scheme shown in Fig. 3. In this setup, a polarizing beam splitter (PB1) divides the initial ultraviolet (UV, wavelength of 263 nm) laser pulse into two pulses according to their polarization. A half-wave plate (HWP) placed in the input beam path allows adjustment of the relative intensity between the two pulses. The pulses are then routed along optical paths of slightly different optical lengths and then recombined using PBS2 resulting in two UV pulse with the relative delay controlled by a motorized translation delay stage. This configuration enables precise tuning of the temporal separation between the two laser pulses and, consequently, between the electron bunches emitted from the photocathode. For our initial tests, we focused on generating two equal-charge bunches, setting the half-wave plate to produce two UV pulses with similar pulse energy.

Following emission, the two bunches were accelerated and transported through the AWA beamline. A spectrometer located downstream of the linac was used to characterize their energy distribution. The energy of the "static" bunch—i.e., the one produced by the *s*-polarized UV pulse—was measured to be E_s = 43.63 MeV. A series of experiments was performed to determine the energy difference between the two bunches as a function of the delay between the *s*- and *p*-polarized UV pulses.

Beam distributions on a dispersive YAG:Ce screen located downstream of the spectrometer were recorded under three conditions: (*i*) static bunch only, obtained by blocking the *p*-polarized "delayed" pulse; (*ii*) delayed bunch only, obtained by blocking the *s*-polarized pulse; and (*iii*) both bunches together. While case (*iii*) would ideally suffice, at small delays the two bunch distributions overlap in the dispersive plane, making it difficult to resolve them. In such cases, the ability to block one pulse or the other improves the measurement resolution. The bunch centroids were determined by fitting Gaussian distributions to the horizontal (dispersive) beam profiles. For the dual-bunch case (*iii*), a double-Gaussian fit was applied to extract the positions of both bunches.

The resulting bunches' energies as function of the optical path difference between the two UV pulses appear in Fig. 4. The static bunch energy remained essentially constants during the scan, while the delayed-bunch exhibited the expected sinusoidal trend. One data point at the extreme negative delay (−15 mm) in both the static-only and dual-bunch scans showed a noticeable deviation from the trend, likely due to temporal drift or shot-to-shot fluctuations.

This data demonstrates that the AWA beamline and optical setup can reliably produce two equal-charge electron bunches with adjustable and stable temporal spacing. Such capability is essential for our upcoming experiment.

CONCLUSION

The preparation of dielectric-lined structures and the implementation of a two-bunch beam configuration at the AWA have been finalized in preparation for an experiment focused on multi-bunch excitation and control of wakefields in dielectric-lined structure. A custom thin-film deposition process was developed and validated to achieve UHV-compatible copper coatings exceeding the target thickness, ensuring effective wakefield confinement for all three structure geometries considered for our experiment. . In parallel, a laser-based pulse-splitting system was designed, implemented, and calibrated to produce two equal-charge electron bunches with controllable and stable separation. The relationship between optical delay arm displacement and bunch separation was established. The experimental is currently in its installation phase.

ISBN: 978-3-95450-261-5 ISSN: 2673-7000 doi: 10.18429/JACoW-NAPAC2025-WEP049

REFERENCES

[1] W. Gai *et al.*, "Experimental demonstration of wakefield effects in dielectric structures", *Phys. Rev. Lett.*, vol. 61, no. 24, pp. 2756–2758, 1988. doi:10.1103/PhysRevLett.61.2756

[2] B. D. O'Shea *et al.*, "Observation of acceleration and deceleration in gigaelectron-volt-per-metre gradient dielectric wakefield accelerators", *Nat. Commun.*, vol. 7, no. 1, p. 12 763, 2016. doi:10.1038/ncomms12763

[3] A. Tremaine, J. Rosenzweig, and P. Schoessow, "Electromagnetic wakefields and beam stability in slab-symmetric dielectric structures", *Phys. Rev. E*, vol. 56, no. 6, pp. 7204–7216, 1997. doi:10.1103/PhysRevE.56.7204

[4] D. Mihalcea, P. Piot, and P. Stoltz, "Three-dimensional analysis of wakefields generated by flat electron beams in planar dielectric-loaded structures", *Phys. Rev. Accel. Beams*, vol. 15, no. 8, p. 081 304, 2012. doi:10.1103/PhysRevSTAB.15.081304

[5] S. Gessner *et al.*, "Design initiative for a 10 TeV pCM wakefield collider", May 2025. https://arxiv.org/abs/2503.20214

[6] A. Zholents *et al.*, "A high repetition rate millimeter wavelength accelerator for an x-ray free-electron laser", *Journal of Instrumentation*, vol. 20, no. 01, p. 01 023, 2025. doi:10.1088/1748-0221/20/01/P01023

[7] P. Piot *et al.*, "Development of a compact light source using a two-beam-acceleration technique", in *Proc. FLS'23*, Luzern, Switzerland, p. pp. 42–45. Aug. 2023. doi:10.18429/JACoW-FLS2023-MO4C2

[8] S. S. Baturin and A. D. Kanareykin, "New method of calculating the wakefields of a point charge in a waveguide of arbitrary cross section", *Phys. Rev. Accel. Beams*, vol. 19. no. 5, p. 051 001, 2016. doi:10.1103/PhysRevAccelBeams.19.051001

[9] B. D. O'Shea *et al.*, "Suppression of deflecting forces in planar-symmetric dielectric wakefield accelerating structures with elliptical bunches", *Phys. Rev. Lett.*, vol. 124, no. 10, p. 104 801, 2020. doi:10.1103/PhysRevLett.124.104801